Study on Temperature Force Control Mechanism of CRTS Ⅱ Slab Track: Control Conditions of Temperature Cracking

Long CHEN, Jinjie CHEN, Jianxi WANG*, Jiasheng CAI, Yang LI

Abstract: Diseases such as track slab arching and joint concrete crushing of China Railway Track System (CRTS)II slab track were caused by huge temperature force, which seriously threatens driving safety of trains. In this study, a longitudinal weak connection scheme of CRTSII slab track was proposed to adjust the temperature force in track slab and reduce diseases of longitudinal continuous track slab. This paper focuses on the cracking characteristics of the longitudinal heterogeneous concrete composite structure. The equation which was originally developed to calculate crack width and structure stress under temperature loads, was put forward to consider deformation difference of different elastic modulus. The influence law of various parameters was analyzed. The reinforcement stress and crack width of CRTSII slab track after longitudinal connection weakening were calculated, and the reasonable limit value of tensile force of connection reinforcement and the minimum value of bond resistance of reinforcement in joint position were obtained. The result shows that, in order to reduce the bond resistance between the joint material and the reinforcement, the elastic modulus of the elastic material should be less than 5000 MPa; in order to ensure that the reinforcement does not produce large stress, the elastic modulus of the joint should be greater than 1000 MPa.

Keywords: arching disease; CRTSII slab track; joint elastic material; temperature cracking; temperature force control

1 INTRODUCTION

CRTSII slab track is a longitudinal continuous ballastless tracks structure which has been applied over 9700 km (extended mileage) in China [1, 2]. CRTSII slab track consists of rail, track slab, cement asphalt (CA) mortar, concrete base (support layer) from top to bottom, shown in Fig. 1. The design of longitudinal continuous ballastless tracks structure, precast concrete track slabs connected by six longitudinal reinforcements and joint post cast concrete, draws lessons from the concept of fixed area of CWR. It is considered that the track slab is continuous and uniform in the longitudinal direction, and there is no expansion and contraction but only temperature force under the action of temperature load. In fact, the wide and narrow joint is the weak position causing the non-uniform longitudinal stiffness of ballastless track [3]. Different degrees of diseases of ballastless track have occurred in operation period, such as interface damage between slab and CA mortar, track slab and wide and narrow joint cracks, track slab arching, joint concrete crushing, etc. [4 ,5], as shown in Fig. 1, which threaten train operation safety [6-9].
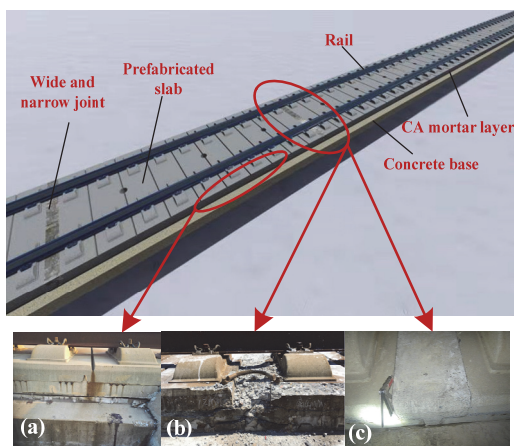
A number of research studies that include theoretical and experimental analysis have been carried out to reveal the disease mechanism. Cohesive zone model, fatigue endurance algorithm (FE-SAFE) and extended finite element methods (XFEM) [10-13] were introduced to analyse the interface damage; then interlayer mix mode cracking analysis model, interface fatigue model were developed based on cohesive model [14, 15], which can further reveal the mechanism of interface damage. Interface test of concrete-CA mortar test block [16, 17] and on-site full scale push slab [18] are conducted to get the interface parameters. The research of structural instability focuses on buckling stability of uniform track slab. Analytical method and energy method [19] were adopted to analyze the buckling modes and buckling loads of different upper arch lines. Finite ešlement model using riks method can consider the non-linearity between layers and the coupling effect with the rail [20-23]. Dai GL et al. [24] measured the initial strength of wide and narrow joint and found that the average strength of wide and narrow joints (45.44 MPa) is less than that of track slab (54.56 MPa). Li DS [25] conducted full scale test of longitudinal stiffness of track slab and concluded that the stiffness of wide and narrow joint is obviously less than that of track slab. The above research shows that the huge temperature force and joint defects are the main causes of these diseases; however, the current research focuses on how the disease is produced rather than how to solve it.

Figure 1 CRTSII slab track and on site damage: (a) track slab arching/interface damage, (b) joint concrete crushing, (c) joint cracks
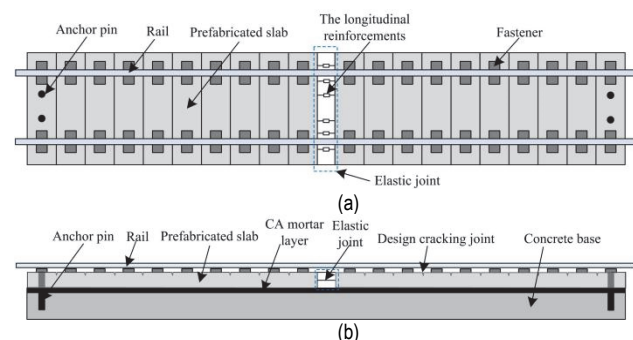

Figure 2 Longitudinal weak connection scheme: (a) top view, (b) side view

In order to better solve the problems of these diseases, a scheme to weaken the longitudinal connection of the track slab is proposed to release the internal temperature force of track slab. In this scheme, the longitudinal track slab is divided into several sections by limiting measures such as planting reinforcement, and the wide and narrow joint concrete in the middle of each segment is replaced by the material with smaller elastic modulus, as shown in Fig. 2, which is called longitudinal weak connection scheme.

Longitudinal connection weakening of track slab will inevitably lead to non-uniformity of longitudinal stiffness and cause the change of track slab cracking characteristics. Although the problems of concrete cracking have been studied, most studies are restricted to longitudinal uniform concrete structure. For example, for concrete pavement structure, Vetter [26] proposed an analytical calculation method for crack spacing of continuously reinforced concrete pavement (CRCP) under temperature load and shrinkage load, which is the basis of reinforcement design and crack calculation of concrete structure. In 1993, American Association of State Highway and Transportation Officials (AASHTO) issued the guide for design of pavement structures [27] based on the observation data of test section. Germany has carried out a lot of research on the temperature stress of ballastless track structure according to the years monitoring temperature statistical data of different regions, and formed a set of design standards for ballastless track structure [28]. In China, Zhao [29] studied the temperature stress method of ballastless track in detail, and deduced the calculation method of temperature stress and crack width of continuous ballastless track. Ren et al. [30] established a calculation model for crack propagation of continuously reinforced concrete slab based on the bond slip theory of reinforced concrete.

In this study, temperature crack calculation method of longitudinal heterogeneous concrete composite structure was proposed. Then the influence law of different parameters was analyzed. Finally, cracking characteristics for longitudinal connection weakening of CRTSII track slab were analyzed, and parameter requirements of joint elastic material were put forward. The result of this study can provide the theoretical guidance for longitudinal weak connection scheme of CRTSII track slab design as well as offer a new computing method for similar problems.

2 LONGITUDINAL HETEROGENEOUS CONCRETE COMPOSITE STRUCTURE CRACK MODEL

The longitudinal weakly connected track slab can be simplified as longitudinal non-uniform concrete composite structure, as shown in Fig. 3. The interaction force between the rail and track slab is much smaller than the cracking axial force of track slab itself, so the restraining effect of the rail fasteners on the track slab is ignored.
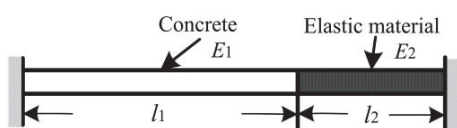
Figure 3 Longitudinal non-uniform concrete composite structure

The elastic moduli of concrete structure and elastic

material are E_1 and E_2 respectively, and $E_1 > E_2$. The lengths of concrete structure and elastic material are l_1 and l_2 respectively. Boundary conditions are considered as clamped end.

The calculation assumptions are as follows: (1) Ignoring the restraint effect between the track slab and CA motor layer. (2) Regardless of the descending stage of the bond slip curve, once the cracks are generated, a through joint will be formed. At this time, only the reinforcement is stressed, and the concrete stress between the cracks is evenly distributed on the cross-section. (3) The bond stress between reinforcement and concrete (elastic material) is a certain value, which is equal to its bond strength. f_b is defined as the bond strength between the elastic material and concrete, f_1 and f_2 are the tensile strength of concrete and elastic material respectively, assuming $f_b < f_2 < f_1$ for the reason that the bond strength of the joint is less than the tensile strength of the material itself in generally.

The generation and development of cracks in non-uniform concrete structures under tension force are shown in Fig. 4. The tensile stress of the structure increases with the increase of the axial force. When the tensile stress increases to the bond strength f_b, cracks are generated at the connection position, the materials on both sides of the crack stops working, and all the tensile force is borne by the reinforcement at the cracking position. The tensile stress of the structure decreases due to the release of partial strain. With the increase of the axial force, when reaching the tensile strength of elastic material, the tensile strength of the structure is reduced when the crack spacing at elastic material position is less than twice the length of the anchorage length of longitudinal reinforcement, new cracks will not be generated with the increase of load. If the axial force of concrete cannot reach its tensile strength under the action of axial force at this time, reinforcement stress and crack width increase rapidly with the increase of axial force. In order to make that the concrete continues cracking under the axial force after cracking at the elastic material position, the stress of the concrete should be greater than its tensile strength, which means, the resistance between elastic material and reinforcement is greater than the axial force when the concrete generates cracks. When the axial load continues to increase to reach the tensile strength of the concrete structure, the concrete structure will begin to crack until a stable crack is formed.
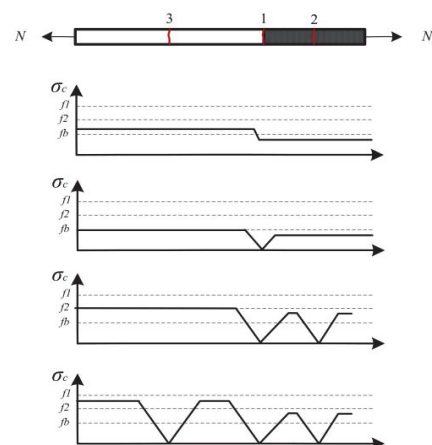
Figure 4 Crack development law of non-uniform track structure

The deformation of reinforcement and concrete is in

accordance with the assumption of plane section, and the stress-strain ratio of reinforcement and concrete increases before reaching the cracking strength of concrete structure. The axial force is:

$$N = N_s + N_c = E_s A_s \varepsilon_{c1} + E_{c1} A_c \varepsilon_{c1} = E_s A_s \varepsilon_{c2} \\ + E_{c2} A_c \varepsilon_{c2} = A_c (n_1 \rho_1 + 1) E_{c1} \varepsilon_{c1} = A_c (n_2 \rho_2 + 1) E_{c2} \varepsilon_{c2} \quad (1)$$

where E_s is elastic modulus of reinforcement, E_{c1} and E_{c2} are elastic moduli of concrete and weak longitudinal connection material respectively, A_s and A_c are section area of reinforcement and concrete respectively, ρ is reinforcement ratio, n_1 and n_2 are elastic moduli ratio of reinforcement to concrete and elastic material, $n_1 = E_s / E_{c1}$, $n_2 = E_s / E_{c2}$.

It can be seen from Eq. (1) that $A_c (n_1 \rho_1 + 1) E_{c1}$ is the tensile stiffness of the concrete and $A_c (n_2 \rho_2 + 1) E_{c2}$ is the tensile stiffness of elastic material. Strain ratio of concrete and elastic material under axial tension force is:

$$\frac{\varepsilon_{c1}}{\varepsilon_{c2}} = \frac{(n_2 \rho_2 + 1) E_{c2}}{(n_1 \rho_1 + 1) E_{c1}} \quad (2)$$

Reinforcement stress is relatively small when tensile stress of joint between concrete and elastic material reaches the bond strength, at this time the tension force is:

$$N_b = N_s + N_c = E_s A_s \varepsilon_{c1} + E_{c1} A_c \varepsilon_{c1} \\ = A_c (n_1 \rho_1 + 1) f_b = A_c (n_2 \rho_2 + 1) f_b \quad (3)$$

The interlayer crack occurs when the axial force reaches N_b which is the bond strength between the elastic material and the concrete, and it no longer conforms to the plane assumption for the materials near the cracked joint. With the axial force increasing, the stress of the reinforcement continues to increase, but the tensile stress of the concrete structure decreases, which is expressed as a peak on the axial force-strain diagram, as shown in Fig. 5. The axial force at the crack position is all borne by the reinforcement:

$$N = E_s A_s \varepsilon = A_s \sigma_s \quad (4)$$

The stress increment of the reinforcement at the crack location is:

$$\Delta \sigma_{s1} = \frac{N_b}{A_s} - \frac{n_1 N_b}{A_c (n_1 \rho_1 + 1)} = \frac{N_b}{A_s} - \frac{n_2 N_b}{A_c (n_2 \rho_2 + 1)} \quad (5)$$
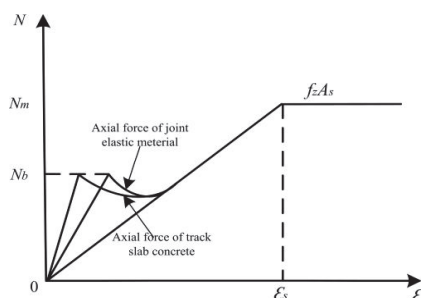
Figure 5 Axial force-strain relationship of longitudinal non-uniform track slab

The crack development law under temperature dropping load is the same as that under tension force. Stress distribution of concrete, elastic material and reinforcement after cracking at the connection position is shown in Fig. 6. The total axial force of the structure is consistent, the strain of the concrete is smaller than that of the elastic material due to the different elastic modulus before cracking of the connection position under the action of temperature dropping load. Therefore, the axial force provided by the concrete reinforcement is less than the axial force of the reinforcement at elastic material position, and the axial force provided by the concrete is greater than the axial force provided by the elastic material.
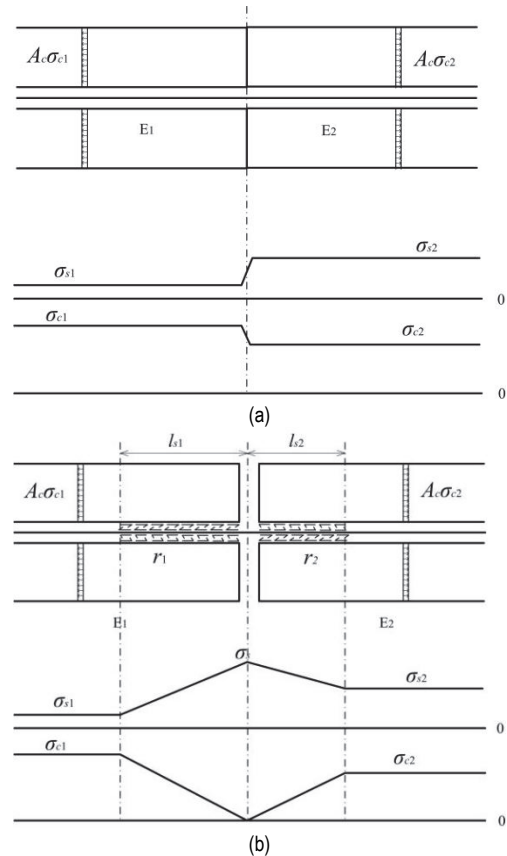
Figure 6 Stress distribution of structure before and after cracking: (a) Before structure cracking, (b) After structure cracking. (σ_{c2} is the stress of elastic material, σ_{s2} is reinforcement stress in elastic material position, σ_s is reinforcement stress in the connection position, r_1 and r_2 are the average viscous resistance between reinforcement and concrete, elastic material respectively, l_{s1} and l_{s2} are anchorage length for concrete structure and elastic structure respectively)

The total axial force is equal under the temperature dropping load which can be obtained as follows:

$$E_{c1}(n_1 \rho_1 + 1) \left(\frac{\alpha \Delta t l_1 - \Delta l_1}{l_1} \right) A = E_{c2}(n_2 \rho_2 + 1) \left(\frac{\alpha \Delta t l_2 - \Delta l_2}{l_2} \right) A \quad (6)$$

where $\Delta l_1 + \Delta l_2 = 0$, $k = \dfrac{l_1}{l_2}$.

Thus:

$$\Delta l_1 = -\Delta l_2 = \frac{(E_{c1} - E_{c2}) l_1 l_2 \alpha \Delta T}{E_{c1}(n_1 \rho_1 + 1) l_2 + E_{c2}(n_2 \rho_2 + 1) l_1} \quad (7)$$

The strain of concrete and elastic material is:

$$\varepsilon_1 = \frac{\Delta l_1}{l_1}, \quad \varepsilon_2 = \frac{\Delta l_2}{l_2} = -\frac{\Delta l_1}{l_2} \tag{8}$$

Thus:

$$\frac{\varepsilon_1}{\varepsilon_2} = -\frac{1}{k} \tag{9}$$

The stress of joint is assumed to be:

$$\sigma_l = \frac{\sigma_{c1} + \sigma_{c2}}{2} \tag{10}$$

When bond strength is fb, Eq. (10) can be expressed as:

$$f_b = \frac{\sigma_{c1} + \sigma_{c2}}{2} \tag{11}$$

Average strain of concrete structure under cooling load ΔT is:

$$
\begin{aligned}
\varepsilon_1 &= \frac{(E_{c1} - E_{c2})l_2}{E_{c1}(n_1\rho_1 + 1)l_2 + E_{c2}(n_2\rho_2 + 1)l_1} \cdot \alpha\Delta T \\
&= \frac{(n_2 - n_1)}{(n_1 n_2 \rho_1 + n_2) + (n_1 n_2 \rho_2 + n_1)k} \alpha\Delta T
\end{aligned} \tag{12}
$$

Average strain of elastic material is:

$$
\begin{aligned}
\varepsilon_2 &= -\frac{(E_{c1} - E_{c2})l_1}{E_{c1}(n_1\rho_1 + 1)l_2 + E_{c2}(n_2\rho_2 + 1)l_1} \cdot \alpha\Delta T \\
&= \frac{(n_1 - n_2)k}{(n_1 n_2 \rho_1 + n_2) + (n_1 n_2 \rho_2 + n_1)k} \alpha\Delta T
\end{aligned} \tag{13}
$$

By substituting Eq. (12) and Eq. (13) into Eq. (11), we obtain the temperature dropping load when the joint cracked.

$$\Delta T = \frac{2 f_b M n_1 n_2}{E_s \alpha \left[(n_1 + n_2)M + (n_1 - n_2)(n_2 - kn_1)\right]} \tag{14}$$

where $M = (n_1 n_2 \rho_1 + n_2) + (n_1 n_2 \rho_2 + n_1)k$.

Average viscous resistance per unit length between reinforcement and concrete is:

$$r_1 = \tau_1 \cdot S \tag{15}$$

where S is surface area of steel per unit length.

For determined reinforcement ratio and reinforcement diameter:

$$S = \frac{4\rho A_c}{d_s} \tag{16}$$

The anchorage length of reinforcement is:

$$l_{s1} = \frac{f_y A_s}{\tau \pi d_s} = \frac{1}{4}\frac{f_y}{\tau} d_s \tag{17}$$

The calculation formula of anchorage length of reinforcement specified in "code for design of concrete" (GB 50010-2010) is:

$$l_{s1} = \alpha_s \frac{f_y}{f_{t1}} d_s \tag{18}$$

Thus the bond strength between reinforcement and concrete is:

$$\tau_1 = \frac{f_{t1}}{4 l_{s1}} d_s \tag{19}$$

So the bond resistance per unit length between reinforcement and concrete can be obtained as:

$$r_1 = \frac{f_{t1} \rho_1 A_c}{l_{s1}} \tag{20}$$

Since the properties of the weak connection material cannot be determined, the bond resistance between the weak connection material and the reinforcement is assumed as r_2.

The relationship between reinforcement stress and concrete stress can be obtained by strain compatibility:

$$
\begin{aligned}
\frac{\sigma_{si}}{E_s} &= \frac{\sigma_{ci}}{E_c}, i = 1, 2 \\
\sigma_{si} &= n_1 \sigma_{ci}, i = 1, 2
\end{aligned} \tag{21}
$$

Take reinforcement and concrete as separate research objects:

$$
\begin{aligned}
r_i l_{si} &= A_{ci} \sigma_{ci} \\
r_i l_{si} &= A_{si}(\sigma_s - \sigma_{si})
\end{aligned} \quad i = 1, 2 \tag{22}
$$

Reinforcement stress at joint position is:

$$\sigma_s = \frac{\sigma_{c1}}{\rho_1} + n_1 \sigma_{c1} = \frac{\sigma_{c2}}{\rho_2} + n_2 \sigma_{c2} \tag{23}$$

The total length of reinforcement remains unchanged for the whole structure under the temperature dropping load with a certain elastic material and a certain length, the tensile length of the reinforcement is equal to the cooling shrinkage:

$$
\begin{aligned}
&\frac{l_1 \sigma_{s1} + l_{s1}(\sigma_s - \sigma_{s1}) + l_2 \sigma_{s2} + l_{s2}(\sigma_s - \sigma_{s2})}{E_s} \\
&= \alpha(l_1 + l_2)\Delta T
\end{aligned} \tag{24}
$$

The change value of reinforcement at concrete position is:

$$\frac{l_{cr1}\sigma_{s1}+l_{s1}(\sigma_s-\sigma_{s1})}{E_s}=\left[1-\frac{(n_2-n_1)}{M}\right]\alpha\Delta Tl_{cr1} \quad (25)$$

And for elastic material position is:

$$\frac{l_{cr2}\sigma_{s2}+l_{s2}(\sigma_s-\sigma_{s2})}{E_s}=\left[1-\frac{(n_1-n_2)k}{M}\right]\alpha\Delta Tl_{cr2} \quad (26)$$

Substituting Eq. (22) and Eq. (23) into Eq. (25) and (26), we can obtain crack spacing for concrete material and elastic material:

$$l_{cr1}=\frac{A_c\sigma_{c1}^2}{r_1\rho_1\left[\left(1-\frac{(n_1-n_2)}{M}\right)\alpha\Delta TE_s-n_1\sigma_{c1}\right]} \quad (27)$$

$$l_{cr2}=\frac{A_c\sigma_{c2}^2}{r_2\rho_2\left[\left(1-\frac{(n_2-n_1)k}{M}\right)\alpha\Delta TE_s-n_2\sigma_{c2}\right]} \quad (28)$$

There will be no more new cracks when the stress σ_{ci} is equal to the tensile strength f_{ti} of the material, the maximum crack spacings for concrete and elastic material are:

$$l_{cr1,\,max}=\frac{A_cf_{t1}^2}{r_1\rho_1\left[\left(1-\frac{(n_1-n_2)}{M}\right)\alpha\Delta TE_s-n_1f_{t1}\right]} \quad (29)$$

$$l_{cr2,max}=\frac{A_cf_{t2}^2}{r_2\rho_2\left[\left(1-\frac{(n_2-n_1)k}{M}\right)\alpha\Delta TE_s-n_2f_{t2}\right]} \quad (30)$$

The maximum crack width at joint position is:

$$w_{l,\max}=\frac{1}{2}l_1[(\alpha\Delta T-\varepsilon_1)-\overline{\varepsilon_{c1}}]+\frac{1}{2}l_2[(\alpha\Delta T-\varepsilon_2)-\overline{\varepsilon_{c2}}] \quad (31)$$

The maximum crack width of each material is:

$$w_{cr,\max}=l_{cri}[(\alpha\Delta T-\varepsilon_i)-\overline{\varepsilon_{ci}}] \qquad i=1,2 \quad (32)$$

The average strain of concrete and elastic material is:

$$\overline{\varepsilon_{ci}}=\frac{\sigma_{ci}(l_{cri}-l_{si})}{E_{ci}l_{cri}} \qquad i=1,2 \quad (33)$$

Reinforcement stress is:

$$\sigma_{si}=E_s(\alpha\Delta T-\varepsilon_i) \quad (34)$$

Stress of concrete and elastic material is:

$$\sigma_{ci}=\frac{\rho\sigma_{si}}{1+\rho_i n} \quad (35)$$

3 PARAMETER ANALYSIS

The above analysis shows that the main parameters affecting the cracking characteristics of non-uniform concrete composite structures are k, n_1 and n_2. It can be seen from Eq. (14) that the corresponding temperature load when the connection position is cracked is proportional to the cracking strength and reinforcement ratio, and inversely proportional to the elastic modulus of the reinforcement. Fig. 7 shows the relationship between k and temperature load when the connection position is cracked. It can be seen that when k is less than 3, as k increases, the temperature load decreases rapidly, and when k is greater than 3, the decreasing trend slows down gradually. It shows that the longer the length of the concrete, the more likely the connection position is to crack; when the ratio of concrete length to elastic material length is greater than 3, cracking temperature is close to that of pure concrete structure. Fig. 8 is the relationship between n_1, n_2 and cracking temperature of connection position, ni is proportional to the cracking temperature; the larger the value of n_1 and n_2, which means the smaller the elastic modulus of concrete and elastic material, the connection position is less likely to crack. The greater the overall rigidity of the concrete and the elastic material, the easier it is to crack.
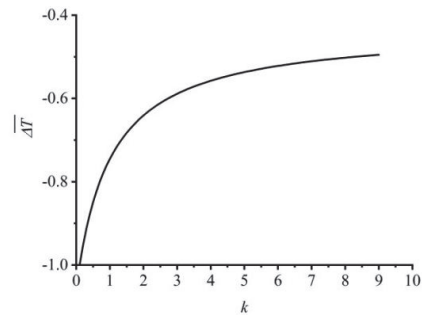

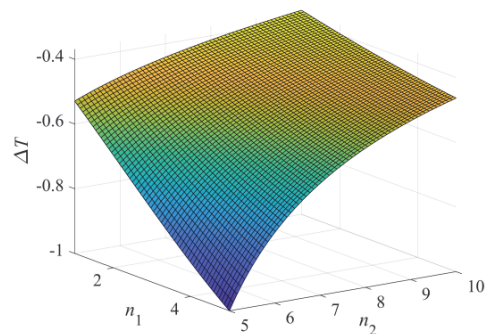
Figure 7 Relationship between k and ΔT

Figure 8 Relationship between n_1, n_2 and ΔT

According to Eq. (29) and Eq. (30), it can be seen that the maximum crack distance is related to the temperature dropping load value and significantly impacted by the elastic modulus of the material. The relationship between the maximum crack spacing and the temperature dropping load when the elastic modulus of the material is constant is analyzed. As shown in Fig. 9, k, which represents the ratio

of l_1 to l_2, has little effect on the maximum crack spacing. Assuming that the temperature dropping load is a constant value, the relationship between different material elastic modulus and the maximum crack width is analyzed, as shown in Fig. 10. The maximum crack spacing of concrete and elastic material is related to elastic modulus ratio of concrete to elastic material. A larger elastic modulus ratio will lead to a larger concrete crack spacing, but a smaller elastic material crack spacing, therefore, the elastic modulus ratio can be determined by the crack spacing index of different materials.
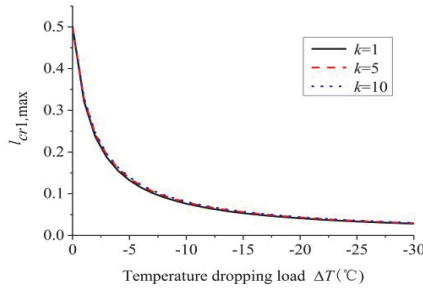

Figure 9 Relationship between cooling load and maximum crack spacing
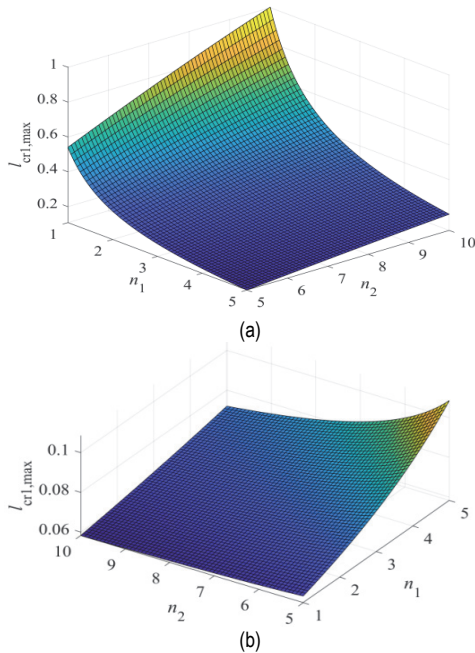

(a)

(b)

Figure 10 Relationship between n_1, n_2 and maximum crack spacing: (a) Crack spacing of track slab, (b) Crack spacing of elastic material.

4 EXAMPLES
4.1 Calculation Conditions and Parameters

The length of connection position l_2 is 0.15 m and the length of track slab l_1 is 6.25 m for CRTSII slab ballastless track. Reinforcement ratio of track slab (ρ_1) is analyzed as 0.75% according to design drawing. Reinforcement ratio of connection position is 0.0062% which is analyzed by six Φ 20 longitudinal reinforcement. The elastic modulus for reinforcement and track slab is 2.05×10^{11} Pa and 3.55×10^{10} Pa, respectively. The elastic models for connection position ranges from 10^8 Pa to 3.55×10^{10} Pa. α_s is 1.6 and reinforcement diameter is 0.01m for track slab, tensile strength of track slab concrete is 1.96 MPa. CRTSII slab ballastless track has been in operation for many years, so the shrinkage load of concrete is not in consideration

and temperature dropping load is considered as −40 ℃. Specific parameters are shown in Tab. 1.

Table 1 Calculation parameters of CRTS Ⅱ slab ballastless track

Parameter	l_1 / m	l_2 / m	E_s / MPa	E_{c1} / MPa	E_{c2} / MPa
Value	6.25	0.15	205000	35500	$100 \sim 35500$
Parameter	ρ_1 / %	ρ_2 / %	α_s	d_s	f_{t1}
Value	0.75	0.006	1.6	0.01	1.96

4.2 Initial Crack Analysis

With the decrease of temperature, crack first occurs at the joint position. According to the Eq. (32), initial crack temperature can be obtained for difference bonding strength and difference connection elastic modulus which are shown in Tab. 2. The max initial crack temperature is 31.92 ℃ when bonding strength is 4 MPa and connection position elastic modulus is 100 MPa which shows the crack occurring at joint position is inevitable.

Table 2 Cracking temperature corresponding to different elastic modulus (−℃)

Tensile strength of joint / MPa	Elastic modulus of elastic material / MPa						
	100	1000	5000	10000	20000	30000	35500
2	15.9	10.5	6.95	6.22	5.82	5.68	5.63
3	23.9	15.8	10.4	9.34	8.73	8.52	8.45
4	31.9	21.1	13.9	12.5	11.6	11.4	11.3

The length of connection position is just 0.15 m, which is far less than the minimum cracking spacing calculated for concrete structure, therefore, it can be considered that the cracking spacing at connection position is equal to the connection position length, $l_m = l_2$, and anchorage length of reinforcement is equal to the length of connection position length, $l_{s2} = l_m = l_2$. Assuming that the resistance per unit length of reinforcement at connection position is r_2, to guarantee the track slab concrete will continue to crack under temperature dropping load after the joint crack occurred, the resistance provided by the connection position after the joint cracks is greater than the axial force of the track slab cracking:

$$r_2 > \frac{f_{t1} A_{c1}}{l_{s2}} \tag{36}$$

The minimum resistance is 6.664×10^6 N/m.
Connection position generates stable cracks when the resistance per unit length of reinforcement is smaller than 6.664×10^6 N/m. After cracks of elastic material occur, the decrease of temperature load leads to the rapid increase of reinforcement stress and crack width at elastic material position.

The corresponding critical temperature dropping load is:

$$\Delta T = \frac{r_2 l_2 M}{E_{c2} A_c \alpha (M - n_2 + n_1)} \tag{37}$$

Fig. 11 shows the relationship between r_2, E_{c2} and ΔT. Critical temperature dropping load value is large when the modulus of elastic material is small. The range of temperature dropping value given in Fig. 10 is $0 \sim -60$ ℃

to make the statement clearer. When the elastic modulus of elastic material is greater than 10000 MPa, the cooling load value increases gradually with the decrease of elastic modulus, but the amplitude is very small. When the elastic modulus is less than 10000 MPa, the temperature dropping load value increases rapidly with the decrease of elastic modulus. The relationship between resistance value and temperature dropping load value is similar to the relationship between elastic modulus of elastic material and temperature dropping load value; the smaller the elastic modulus of elastic material, the larger the amplitude of temperature dropping load value caused by the change of resistance value. According to the junction position of two curved surfaces in the figure, the minimum resistance value corresponding to the different elastic modulus of elastic material can be obtained when the temperature dropping load value is 40 °C, as shown in Tab. 3. In order not to produce stable cracks, the elastic modulus of elastic material should be less than 10000 MPa when the resistance value is critical resistance.
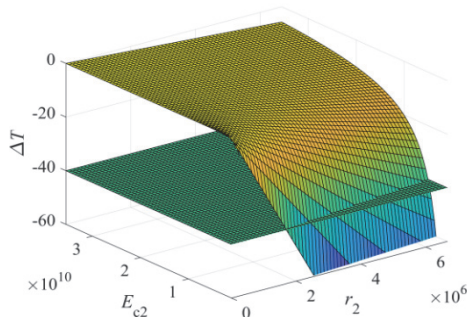

Figure 11 Relationship among r_2, E_{c2} and cooling load

Table 3 Minimum resistance value between reinforcement and elastic material without stable crack

E_{c2} / MPa	r_2 / N
100	8.96×10^4
1000	1.03×10^6
5000	6.12×10^6

When $r_2 > 6.664 \times 10^6$ N/m and only connection position cracks, crack width with different elastic modules of elastic material in −40 °C of temperature dropping load can be obtained according to Eq. (32) and is shown in Fig. 12. The calculation result shows that the smaller the elastic modulus of elastic material and the lager the crack spacing the lager the crack width in connection position. The crack width is about 0.1 mm when elastic modulus of elastic material is equal to concrete elastic modulus.
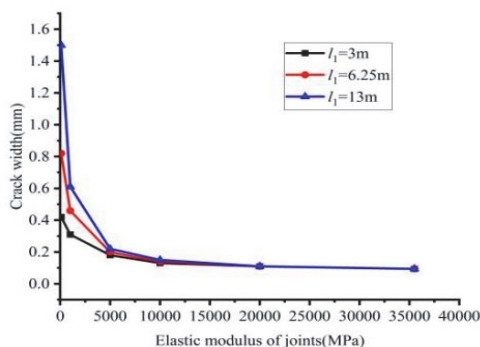

Figure 12 Crack width of different crack spacing at connection position

The crack width is 1.5 mm which cannot meet the design requirements when the crack spacing is 13m and elastic modulus of elastic material is 100 MPa.

4.3 Crack Analysis of Track Slab After Cracking

Track slab cracks begin to occur after the connection position cracks with the increase of axial force and gradually develop into stable cracks. As the track slab is provided with pre-cracks to guide the development of cracks, crack spacing can be taken as the width between two pre-cracks, $l_m = 0.65$ m. Crack width of connection position and track slab can be obtained according to Eq. (31) and Eq. (32) respectively, the result is shown in Fig. 13. The crack width of track slab decreases with the decrease of elastic modulus of elastic material, the crack width of track slab is 0.14 mm and the crack width at the connection position is 0.03 mm when the elastic modulus of elastic material is 35500 MPa. The crack width at the connection position increases with the decrease of elastic modulus of elastic material, but the range of change is very small, the maximum crack width and minimum crack width are 0.1 mm and 0.092 mm respectively. Therefore, the decrease of elastic modulus of elastic material can effectively reduce the crack width of track slab.

The structure stress which is shown in Fig. 14 and Fig. 15 with −40 °C of temperature dropping load can be calculated according to Eq. (35) and Eq. (36). The stress of track slab reinforcement gradually increases from 3.3 MPa to 60 MPa with the increase of elastic modulus.
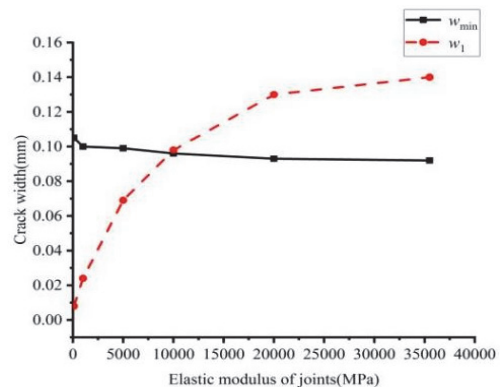

Figure 13 Crack width of track slab and joint position
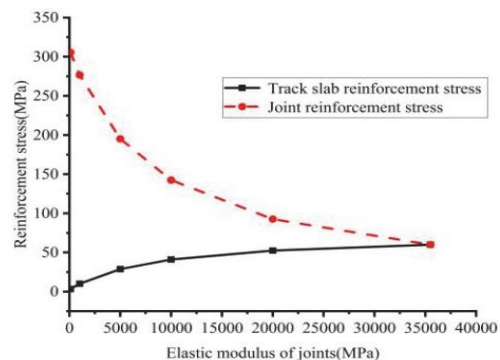

Figure 14 Reinforcement stress

However, with the increase of elastic modulus, the reinforcement stress in elastic material position decreases from 305.5 MPa to 60 MPa gradually; the calculated value of reinforcement stress is 286 MPa, which does not meet

the design requirements when the elastic modulus of elastic material is 100 MPa. The stress of track slab concrete increases from 0.024 MPa to 0.432 MPa gradually with the increase of elastic modulus. The material stress of elastic material is very small, which is reduced from 0.016 MPa to 0.004 MPa.
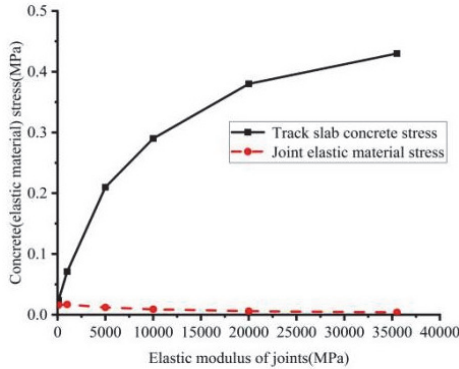

Figure 15 Stress of track slab and elastic material

After the track slab cracks, the overall tensile stiffness decreases. Research shows that under the common crack spacing of 1 ~ 2 m, the reduced stiffness after cracking is about 2 ~ 3 times that of the design stiffness of the track slab. Now take the stiffness reduction factor of 0.5 to calculate the crack width and reinforcement stress. The comparison results are shown in Tab. 4. It can be seen that when the reduction factor is 0.5, the crack width of track slab increases slightly, but it is far less than the calculated value. The reinforcement stress in elastic material position is reduced by about 40 MPa. The results show that the calculated results according to the design elastic modulus of track slab are conservative.

Table 4 Comparison of reinforcement stress and crack width with different stiffness reduction factor

Elastic modulus of joint / MPa	Reinforcement stress in track slab position / MPa		Reinforcement stress in joint position / MPa		Crack width at joint position / mm		Crack width of track slab / mm	
	Reduction factor 1	Reduction factor 0.5	Reduction factor 1	Reduction factor 0.5	Reduction factor 1	Reduction factor 0.5	Reduction factor 1	Reduction factor 0.5
100	3.34	6.34	305.5	292.5	0.105	0.105	0.008	0.015
1000	9.98	17.48	276.7	244.2	0.1	0.102	0.024	0.042
5000	28.8	41.32	195.1	140.9	0.099	0.096	0.069	0.099
10000	40.97	52.58	142.48	92.17	0.096	0.093	0.098	0.126
20000	52.48	61.27	92.57	54.48	0.093	0.091	0.13	0.147
35500	60	66.2	60	33.3	0.092	0.09	0.14	0.158

4.4 Analysis of Reasonable Tensile Force Value

Longitudinal connection reinforcement at elastic material position needs to be tensed during the construction process. When considering the tensile force of reinforcement, the stress of reinforcement at weak connection position should be:

$$\sigma_{s,z} = \sigma_{s2} + \frac{N_z}{A_s} \tag{38}$$

The calculated value of reinforcement stress is 286 MPa. According to Eq. (38), the maximum tensile force of each reinforcement corresponding to different elastic modulus of elastic material can be obtained, as shown in Tab. 5.

Table 5 The maximum tensile force corresponding to steel stress checking

Elastic modulus of elastic material / MPa	Maximum tensile force of longitudinal reinforcement / kN
100	-
1000	2.92
5000	28.4
10000	45.1
20000	60.7
35500	70.9

After applying N_z tensile force to each connection reinforcement, the track slab is subjected to $6N_z$ (there are 6 connection reinforcements in total) tensile force, which is equivalent to temperature dropping load:

$$\Delta T_z = \frac{6N_z}{E_{c1}\alpha(n_1\rho_1 + 1)} \tag{39}$$

The track slab crack width is:

$$w_{cr1,z} = l_{cr1}\left\{ \left[(\alpha\Delta T + \alpha\Delta T_z) - \varepsilon_1 \right] - \overline{\varepsilon_{c1}} \right\} \tag{40}$$

The relationship between tensile force value and crack width of track slab can be obtained by Eq. (39) and Eq. (40), as shown in Tab. 6. The maximum tensile force of each reinforcement corresponding to different elastic modulus can be obtained when the crack width $w_{cr1,z}$ is 0.5 mm (maximum crack width specified in the specification).

Table 6 The maximum tensile force corresponding to crack width checking

Elastic modulus of elastic material / MPa	Maximum tensile force of longitudinal reinforcement / kN
100	53.7
1000	51
5000	46.2
10000	42.8
20000	39.7
35500	38.7

The maximum tensile force value corresponding to different elastic modulus can be obtained by taking the minimum value of tensile force in Tab. 5 and Tab. 6, as shown in Tab. 7. It can be seen that when the elastic modulus of elastic material is less than 10000 MPa, the

maximum tensile force value is controlled by the stress of reinforcement in elastic material position, but when the elastic modulus is greater than 10000 MPa, the tensile force value is controlled by the crack width of track slab.

Table 7 Maximum tensile force limit of longitudinal reinforcement corresponding to different joint elastic modulus

Elastic modulus of elastic material / MPa	Maximum tensile force of longitudinal reinforcement / kN
100	-
1000	2.92
5000	28.4
10000	42.8
20000	39.7
35500	38.7

5 CONCLUSIONS

In this paper a longitudinal connection weakening scheme of CRTSII slab track was proposed to reduce arching disease of track slab. The calculation method of cracks and temperature force of longitudinal heterogeneous concrete composite structure was put forward. The influence law of various parameters was analyzed. The reinforcement stress and crack width of CRTSII slab track after longitudinal connection weakening are calculated, and the reasonable limit value of tensile force of connection reinforcement and the minimum value of bond resistance of reinforcement in elastic position are obtained. Specific conclusions are as follows:

(1) For longitudinal heterogeneous track slab concrete composite structure, when the connection position cracks, the longer the elastic material length, the less likely the joint position is to crack. When the ratio of elastic material length to concrete length is greater than 1/3, the cracking temperature will be significantly increased. The larger the overall stiffness ratio between track slab and elastic material, the easier the joint position is to crack.

(2) For CRTSII slab track structure, the track slab will crack only when the bonding resistance per unit length between reinforcement and elastic material is larger than 6.664×10^6 N/m.

(3) When the bonding resistance between reinforcement and elastic material is large enough, the smaller the elastic modulus, the larger the crack width, the larger the crack spacing and the larger the crack width. Under normal working conditions, that is, when the elastic modulus of weak connection position is equal to the elastic modulus of track slab, the crack width is about 0.1 mm. When the crack spacing is 6.25 m and 13 m, the maximum crack width is 0.83 mm and 1.5 mm respectively, which cannot meet the design requirements. When the maximum crack spacing is 3 m, the maximum crack width does not exceed 0.5 mm, which can meet the design requirements.

(4) After the track slab cracks, the decrease of elastic modulus of elastic material can effectively reduce the crack width of track slab, but increase reinforcement stress at elastic material position. When the elastic modulus of elastic material is less than 100 MPa, the reinforcement stress is 306 MPa, which cannot meet the design requirements.

6 REFERENCES

[1] Liu, Y., Xu, Q., Sun, X., Yang, G., & Zhao, G. (2021). Simulation of delamination evolution of slab ballastless track under vertical impact. *Shock and Vibration*, *2021*, 1-13. https://doi.org/10.1155/2021/4022875

[2] Szurgott, P. & Bernacki, P. (2020). Modelling of steel-concrete bridges subjected to a moving high-speed train. *International Journal of Simulation Modelling*, *19*(1), 29-40. https://doi.org/10.2507/IJSIMM19-1-499

[3] Liu, X., Zhang, W., Xiao, J., & Liu, X. (2019). Damage mechanism of broad-narrow joint of CRTSII slab track under temperature rise. *KSCE Journal of Civil Engineering*, *23*(5), 2126-2135. https://doi.org/10.1007/s12205-019-0272-2

[4] Li, Y., Chen, J., Wang, J., & Shi, X. (2020). Analysis of damage of joints in CRTSII slab track under temperature and vehicle loads. *KSCE Journal of Civil Engineering*, *24*(4), 1209-1218. https://doi.org/10.1007/s12205-020-1799-y

[5] Cai, X., Luo, B., Zhong, Y., & Zhang, Y. (2019). Arching mechanism of the slab joints in CRTSII slab track under high temperature conditions. *Engineering Failure Analysis*, *98*, 95-108. https://doi.org/10.1016/j.engfailanal.2019.01.076

[6] Ren, J., Deng, S., Jin, Z., & Yang, J. (2017). Energy method solution for the vertical deformation of longitudinally coupled prefabricated slab track. *Mathematical Problems in Engineering,* 8513240. https://doi.org/10.1155/2017/8513240

[7] Yang, Y., Yuan, Z., & Meng, R. (2022). Exploring traffic crash occurrence mechanism toward cross-area freeways via an improved fata mining approach. *Journal of Transportation Engineering Part A Systems*, 148(9), 04022052. https://doi.org/10.1061/JTEPBS.0000698

[8] Yang, Y., Yuan, Z., Chen, J., & Guo, M. (2017). Assessment of osculating value method based on entropy weight to transportation energy conservation and emission reduction. *Environmental Engineering & Management Journal*, 16(10), 2413-2424. https://doi.org/10.30638/eemj.2017.249

[9] Yang, Y., He, K., Wang, Y., Yuan, Z., & Yin, Y. (2022) Identification of dynamic traffic crash risk for cross-area freeways based on statistical and machine learning methods. *Physica A: Statistical Mechanics and its Applications*, *595*(2022), 127083. https://doi.org/10.1016/j.physa.2022.127083

[10] Zhu, S. & Cai, C. (2013). Interface damage and its effect on vibrations of slab track under temperature and vehicle dynamic loads. *International Journal of Non-linear Mechanics*, *58*, 222-232. https://doi.org/10.1016/j.ijnonlinmec.2013.10.004

[11] Zhong, Y., Gao, L., & Zhang, Y. (2018) Effect of daily changing temperature on the curling behavior and interface stress of slab track in construction stage. *Construction and Building Materials*, *185*, 638-647. https://doi.org/10.1016/j.conbuildmat.2018.06.224

[12] Premrov, M., Ber, B., & Kozem Silih, E. (2021). Study of load-bearing timber-wall elements using experimental

testing and mathematical modelling. *Advances in Production Engineering & Management*, 16(1), 67-81. https://doi.org/10.14743/apem2021.1.385

[13] Xiao, H., Zhang, Y., Li, Q., & Feng, J. (2019). Analysis of the initiation and propagation of fatigue cracks in the CRTS II slab track inter-layer using FE-SAFE and XFEM. *Proceedings of the Institution of Mechanical Engineers, Part F: Journal of Rail and Rapid Transit*, 233(7), 1-13. https://doi.org/ 10.1177/0954409718805296

[14] Zhang, J., Zhu, S., Cai, C., & Wang, M. (2020). Experimental and numerical analysis on concrete interface damage of ballastless track using different cohesive models. *Construction and Building Materials, 263*, 120859. https://doi.org/10.1016/j.conbuildmat.2020.120859

[15] Zhong, Y., Gao, L., & Zhang, Y. (2018). Effect of daily changing temperature on the curling behavior and interface stress of slab track in construction stage. *Construction and Building Materials*, 185, 638-647. https://doi.org/10.1016/j.conbuildmat.2018.06.224

[16] Liu, Y., Xu, Q., Sun, X., & Yang, G. (2021). Push plate test of CRTS II slab ballastless track: theoretical analysis, experiments, and numerical simulation. *Shock and Vibration,* 1945385. https://doi.org/10.1155/2021/1945385

[17] Liu, X., Liu, X., Xiao, J., & Di, Y. (2018). Vertical stability of longitudinal continuous ballastless track under temperature variation. *Journal of Southwest Jiao Tong University*, 53(5), 921-927.

[18] Dai, G. & Su, M. (2016). Full-scale field experimental investigation on the interfacial shear capacity of continuous slab track structure. *Archives of Civil and Mechanical Engineering*, 16(3), 485-493. https://doi.org/10.1016/j.acme.2016.03.005

[19] Chen, Z., Liu, X., Xiao, J., & Zhang, W. (2021). Comprehensive analysis of stability and strength of CRTSII slab track with up-warp deformation. *Journal of The China Railway Society*, 43(6), 112-120.

[20] Yang, Y., Tian, N., Wang, Y., & Yuan, Z. (2022) A parallel FP-Growth mining algorithm with load balancing constraints for traffic crash data. *International Journal of Computers Communications & Control*, 17(4), 4806. https://doi.org/10.21203/rs.3.rs-1311180/v1

[21] Hossain, M. (2019). IPS & PPVC precast system in construction- a case study in singaporean housing building project. *Journal of System and Management Sciences*, 9(2), 23-42.

[22] Li, P. (2015) *Analysis of the interface damage of CRTSII slab track and its influences*. Southwest Jiaotong University, Chengdu, China.

[23] Yang, Y., Wang, K., Yuan, Z., & Liu, D. (2022). Predicting freeway traffic crash severity using XGBoost-Bayesian network model with consideration of features interaction. *Journal of Advanced Transportation*, 4257865. https://doi.org/10.1155/2022/4257865

[24] Dai, G. & Ge, H. (2020). Statistical analysis of the initial state characteristics of the longitudinally connected ballastless track on bridge. *Journal of Railway Engineering Society*, 264(9), 1-6.

[25] Li, D. (2016). *Performance of CRTSII slab ballastless track on the high speed railway bridge*. China Academy of Railway Sciences, Beijing, China.

[26] Vetter, C. & Asce, A. M. (1933). Stresses in reinforced concrete due to volume changes. *Transactions of the American Society of Civil Engineers*, 98(2), 1039-1053. https://doi.org/10.1061/TACEAT.0004490

[27] American Association of State Highway and Transportation Officials (AASHTO) (1993). Guide for design of pavement structures. Washington, D.C.

[28] DeutschesInstitut Fur Normung. (2001). Concrete, Reinforced and Prestressed Concrete Structures-Part 1: Design and Construction, DIN 1045-1-2001; Berlin, Germany.

[29] Zhao, P. (2008). *Research on the design theory and method for ballastless track on passenger dedicated line*. Southwest jiaotong university, Chengdu, China.

[30] Ren, J., Liu, X., & Zhao, P. (2010). Crack calculation method and influence factors for continuously reinforced slab. *Journal of Southwest Jiao Long University*, 45(1), 34-38+44.

Contact information:

Long CHEN, PhD
State Key Laboratory of Mechanical Behavior and System Safety of Traffic Engineering Structures & Key Laboratory of Roads and Railway Engineering Safety Control,
Ministry of Education,
Shijiazhuang Tiedao University,
Shijiazhuang, Hebei, China, 050043
E-mail: chen0244@163.com

Jinjie CHEN, PhD, Professor
Key Laboratory of Roads and Railway Engineering Safety Control,
Ministry of Education,
Shijiazhuang Tiedao University,
Shijiazhuang, Hebei, China, 050043
E-mail: cjjwxq@126.com

Jianxi WANG, PhD, Professor
(Corresponding Author)
State Key Laboratory of Mechanical Behavior and System Safety of Traffic Engineering Structures,
Shijiazhuang Tiedao University,
Shijiazhuang, Hebei, China, 050043
E-mail: qianxi-2008@163.com

Jiasheng CAI, PhD, Candidate
Key Laboratory of Roads and Railway Engineering Safety Control,
Ministry of Education,
Shijiazhuang Tiedao University,
Shijiazhuang, Hebei, China, 050043
E-mail: 244047187@qq.com

Yang LI, PhD, Candidate
Key Laboratory of Roads and Railway Engineering Safety Control,
Ministry of Education,
Shijiazhuang Tiedao University,
Shijiazhuang, Hebei, China, 050043
E-mail: laolitougao@126.com